Viscous Sintering Phenomena in Liquid−Liquid Dispersions: Application to the Preparation of Silicone Macroporous Aerogels

F. Placin,[†] M. Feder,[‡] and F. Leal-Calderon*[,§]

Centre de Recherche Paul Pascal, Centre National de la Recherche Scientifique, Avenue Albert Schweitzer, 33600 Pessac, France, Rhodia Silicones, 55 Rue des frères Perret, 69191 St Fons Cedex, France, and Laboratoire des milieux dispersés alimentaires, ISTAB, Avenue des facultés, 33405 Talence, France

Received: December 6, 2002; In Final Form: June 13, 2003

When a rupturing agent is added to a stable emulsion made of highly viscous droplets, a gel forms, which further contracts, preserving the geometry of the container (Philip, J.; et al. *Phys. Rev. Lett.* **2000**, *84*, 2018). This phenomenon termed "homothetic contraction" is reminiscent of the classical sintering phenomena occurring during the densification of ceramics, aerogels, etc. The pioneering observation of Philip et al. demonstrates that viscous sintering can occur in organic materials having much lower viscosity than solid inorganic particles in ceramics and glasses (6−8 orders of magnitude smaller). In this paper we exploit the homothetic contraction of silicone-in-water emulsions to produce macroporous aerogels. We describe the procedure employed for the preparation and we characterize the aerogels by SEM and porosity measurements. We discuss the potential applications of the obtained aerogels.

I. Introduction

Liquid−liquid dispersions are observed in numerous systems such as emulsions or phase separating binary fluid mixtures. These systems tend to coarsen in time via two limiting mechanisms. The first one termed as Ostwald ripening is due to the molecular diffusion of the dispersed phase trough the continuous phase.[1] This mechanism does not involve film rupturing: instead, there is transfer of matter from the smaller to the larger dispersed droplets. When the two phases are poorly miscible, coarsening is only due to coalescence phenomena.[2] Coalescence consists of the rupture of the thin liquid film between two adjacent droplets through the nucleation of a small channel. This first nucleation step is followed by a shape relaxation driven by surface tension, which causes two droplets to fuse into a single one. The characteristic time for shape relaxation is governed by the competition between surface tension and viscous dissipation and is given by $T_r \propto \eta R/\gamma$, where η is the viscosity of the droplets, R is their characteristic radius, and γ is their surface tension.[3] When there is no energy barrier for coalescence, the droplets coalesce as soon as they collide. This nonactivated coarsening has been identified in the late stages of phase separations or in strongly unstable emulsions. The limit that was most extensively studied to date corresponds to systems in which the characteristic shape relaxation time T_r is shorter compared to the time T_b separating two droplet collisions (under the effect of brownian motion). In this limit, it was found both theoretically and experimentally that the average droplet size scales with time t as $t^{1/3}$ in 3-D systems.[4] A very different scenario has been recently observed in the limit where T_r is much larger than T_b.[5] In this situation, the coarsening is limited by shape relaxation, leading to very different structures and kinetics than in the previous case. This limit is frequently encountered in systems such as emulsions of highly viscous substances (asphalt, colophon) or phase separations in binary mixtures of polymer. Philip et al.[5] have explored the coarsening mechanisms in fluid−fluid mixtures in the limit where $T_r \gg T_b$. They use model emulsions of highly viscous oils (asphalt, colophon oil) that can be made suddenly unstable toward coalescence upon addition of a suitable chemical. Once the emulsion is made unstable, the droplets form a macroscopic gel made of an array of fused droplets. Then the gel continuously contracts with time to reduce its surface area.

This contraction phenomenon is reminiscent of the sintering process observed in ceramics and aerogels.[6−8] It has been known for a quite long time that powders made of fine packed particles can be sintered at temperatures well below the melting point of the same macroscopic solid phase. During sintering, the materials become tougher or denser by reducing the total surface area. In the case of gels and glasses, the sintering occurs due to viscous flow of matter, whereas in ceramics and metals it could be due to evaporation, surface diffusion, and viscous flow. This phenomena has been widely used for the production of dense ceramics materials from powders, the manufacturing of refractory materials at low temperatures, the coating of electronic components and optics, etc.

In this paper, we present experimental evidence for viscous sintering phenomena in a gel formed by silicone emulsion droplets. When salt is added to the initially stable emulsion, it forms a gel, which contracts with time by preserving the geometry of the container. Therefore, the observed contraction phenomena is identical to the one observed by Philip et al.[5] By properly choosing the rupturing agent and the degree of cross-linking of the silicone chains, we are able to stop the shape relaxation process at the early stages of contraction. This allows getting a bicontinuous material with connected pores. The water is eliminated by sublimation and we finally obtain a light macroporous aerogels. We characterize the structure using SEM and porosity measurements. Finally, we discuss the potential applications of the obtained materials.

* Corresponding author. Tel: 33 6 84 84 51 82. E-mail: f.leal@istab.u-bordeaux1.fr.
[†] Centre National de la Recherche Scientifique.
[‡] Rhodia Silicones.
[§] ISTAB.

10.1021/jp022544o CCC: $25.00
Published on Web 07/29/2003

II. Sample Preparation

The system used as a precursor to prepare macroporous aerogels is a silicone-in-water emulsion. The emulsion is stable over years in standard storage conditions. To produce a macroporous gel, we introduce in the continuous phase a rupturing agent, i.e., a chemical species that produces coalescence and gelation of the droplets. The gel will contract under the effect of surface tension, thus providing a bicontinuous material. Because the process of contraction can be arrested, we obtain a light macroporous aerogel after elimination of the water phase. In this section, we describe the process step by step.

(1) Emulsification. We first produce an oil-in-water monodisperse emulsion stabilized by sodium dodecyl sulfate (SDS). The oil phase is a mixture of silicone oil (48V135000 from Rhodia), resin (4509, Rhodia), and stannic catalyst (metatin 812, from Rhodia). Typically, 100 g of silicone oil are mixed with 7 g of resin and 0.5 g of catalist. To produce the emulsion, the oil phase is gently stirred in the presence of 10 g of a water phase containing 30% in weight of SDS (from Aldrich). Under the effect of shear and in the presence of SDS molecules, the oil phase is fragmented into large droplets ($1-100\ \mu$m) dispersed in the water phase. This crude polydisperse emulsion is fragmented again to get an emulsion with reduced droplet size and polydispersity. A Couette-type mixer consisting of two concentric cylinders was used for that purpose. A scheme of the setup is available in ref 9. The inner cylinder of radius $r \approx 20$ mm is moved by a motor that rotates at a selected angular velocity ω which can reach up to 70 rad·s^{-1}. The outer cylinder is immobile. The gap between the stator and the rotor is fixed to $e = 100\mu$m. For the maximum angular velocity, we are able to reach very high shear rates $\dot{\gamma} \approx r\omega/e = 14\ 200\ \text{s}^{-1}$ in simple shear flow conditions. The premixed crude emulsion is pushed into the gap between the rotor and the stator by means of a piston and the residence time of the emulsion inside the mixer gap is of the order of 10s. After the fragmentation process, the SDS concentration with respect to the continuous phase is always fixed at 10^{-2} mol/L and the oil droplet volume fraction is set to 10%. This is obtained by centrifugating the emulsion right after its fragmentation, removing the continuous phase and replacing it by a surfactant solution at concentration 10^{-2} mol/L. This washing procedure was repeated at least three times to set precisely the composition at the desired value. The emulsion obtained after centrifugation was perfectly stable over a period of months.

The droplets size was measured using a Malvern Particle sizer (Mastersizer S). The collected scattered intensity as a function of the angle is transformed into the size distribution using the Mie theory. The mean droplet diameter in volume D(4,3) is defined as

$$D(4,3) = \frac{\sum_i N_i D_i^4}{\sum_i N_i D_i^3}$$

where Ni is the total number of droplets with diameter D_i. The polydispersity of the emulsion is characterized by a parameter termed as "uniformity" and defined as

$$U = \frac{1}{\bar{D}} \frac{\sum_i N_i D_i^3 |\bar{D} - D_i|}{\sum_i N_i D_i^3}$$

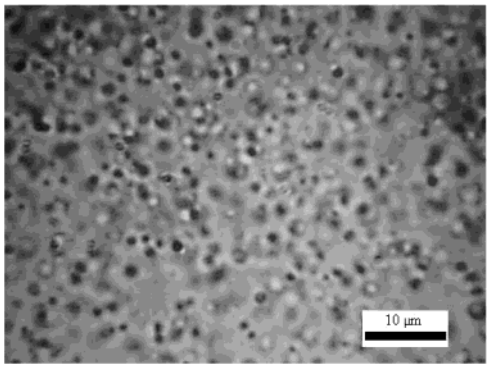

Figure 1. Microscopic image of a typical emulsion obtained with a phase contrast optical microscope (Axiovert ×100). The mean droplet size is around 1 μm, and the uniformity is close to 30%.

where $\bar{D}$ is median diameter, i.e., the diameter for which the cumulative undersized volume fraction is equal to 50%. In Figure 1 we report the image of a typical emulsion obtained with a phase contrast optical microscope (Axiovert ×100). The mean droplet size is around 1 μm and the uniformity is close to 30%.

(2) Silicone Polymerization and Cross-Linking. Right after the emulsification process, the low shear viscosity of the oil droplets is close to 200 Pa·s, a value which is sufficiently small to allow easy fragmentation of the droplets in the previously defined conditions. However, this value can be considered as insufficient to induce gelation and further homothetic contraction of the emulsion. Indeed, from ref 5, we learn that the shape relaxation of a gel made of interconnected droplets is kinetically controlled by the viscous flow of matter within the oil phase. Assuming that the surface energy loss per unit time is equal to the rate of viscous dissipation, a simple model[10−12] predicts that volume fraction ϕ of oil in the contracting gel varies nearly linearly with time for $10\% < \phi < 80\%$, with a slope proportional to the inverse viscosity of the droplets. This theoretical prediction was experimentally verified by Philip et al.[5] The same authors also demonstrated that if the droplet aggregation is diffusion limited, the homothetic contraction is observed when the viscosity of the dispersed phases is larger than approximately 1000 Pa·s.

In our system, the oil droplets are composed of macromolecular silicone chains. To increase the viscosity up to the limiting value of 1000 Pa·s, we produce further polycondensation and cross-linking of the chains. This was achieved in the presence of the resin which was initially mixed with silicone. To be operative, oil and resin have to be in contact with stannic salt which acts as a catalyst. The condensation reaction is delayed and occurs within a few days. We allowed the reaction to take place at room temperature ($T = 20$ °C) for 1 week. This long period was found to be necessary to get droplets with sufficiently high viscosity.

(3) Emulsion Gelation and Shape Relaxation. We now describe the way we produced emulsion destabilization and homothetic contraction. For this scenario to occur, the droplets must irreversibly aggregate much faster than shape relaxation takes place. Thus, the destabilization process must be as fast as possible and must be spatially homogeneous. Following the pioneering work of Poulin et al,[13,14] we introduce in the continuous phase 0.2 mol/L of potassium iodide (KI, from Aldrich) at 65 °C. At such a high temperature, the droplets are perfectly dispersed and kinetically stable, allowing a perfect homogenization of the salt. Then the sample is cooled and below the critical temperature of 40 °C, the droplets become strongly

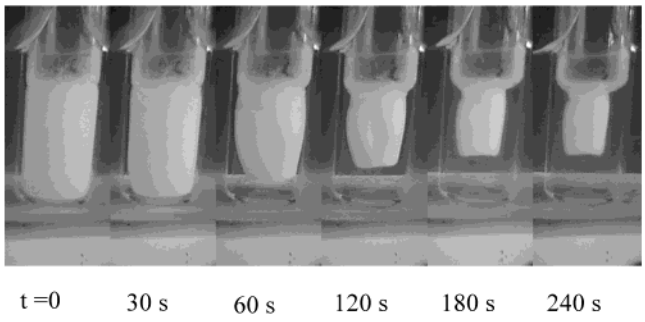

Figure 2. Microscopic evolution of the gel contraction after quenching the sample from 65 °C to room temperature (20 °C). Initial gel volume fraction =10%.

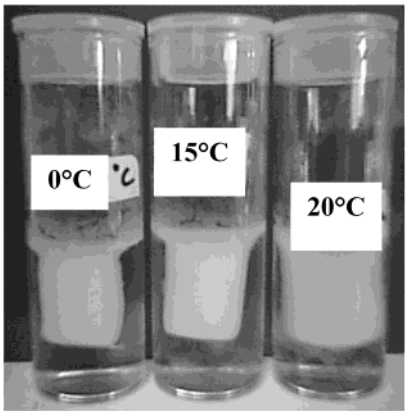

Figure 3. Aspect of the final gel quenched at different temperatures: (a) 0 °C; (b) 15 °C; (c) 20 °C. In all cases, the initial oil volume fraction of the emulsion was 10% and the KI concentration was 0.2 mol/L. The mean droplet diameter was 1 μm. The emulsion was prepared at 65 °C. Then, the sample was dipped in a water solution at one of the three temperatures.

aggregated. The droplets are submitted to a diffusion-limited process of aggregation at the end of which a tenuous gel is formed. As was reported by Poulin et al,[13−15] the presence of alkaline ions such as Li^+, Na^+, or K^+ produces precipitation of the dodecyl sulfate molecules. For the same reasons, droplets covered by the same surfactant molecules become strong adhesives at the approach of the precipitation temperature. It was noticed[15] that K^+ produced not only adhesion but also coalescence between the droplets. This is the reason this ion was preferred to the other ones.

Once this network is formed, the gel starts to contract by reducing its surface area. In this process water is expelled from the space filling network. In Figure 2, we show the evolution of the gel contraction after quenching the sample in a ice bath (0 °C). The contraction remains remarkably homothetic, meaning that it preserves the geometry of the container. We have verified this point by performing experiments in a variety of containers such as rectangular or cylindrical containers. Figure 3 shows the aspect of the final gel quenched at different temperatures: 0 °C in ice bath, 15 °C in a water bath, and 20 °C in air. In all cases, the initial oil volume fraction of the emulsion was 10% and the KI concentration was 0.2 mol/L. The mean droplet diameter was 1 μm. Typically, 2 cm^3 of emulsion are prepared in a cylindrical vessel at 65 °C. Then, the sample is dipped in a water solution at one of the three previously mentioned temperatures. We observe that quenching the sample at lower temperature has the effect to produce a denser gel, i.e., with higher final silicone volume fraction ϕ. By measuring the final dimensions of the gel, we can deduce ϕ and find that it varies between approximately 20% and 30% in the explored temperature range.

Here arise the questions to know why the gel contraction is arrested at such low ϕ values and why the final state of the gel is dependent upon the final temperature of the quench. The fact that the contraction is stopped at relatively low ϕ can be considered as surprising regarding the results of Philip et al.[5] Indeed, in the presence of highly viscous asphalt droplets, these authors found that the final gel reaches 90% to 95% in volume fraction. In our case, we believe that the silicone droplets are partially solid as a result of cross linking. In other words, it is probable that solid parts coexists with fluid ones inside the silicone network. Because the solid fraction cannot flow, it forms a kind of rigid structure in the gel that may arrest the contraction. Because the surfactant also precipitates, it also forms a rigid network that may influence the contraction. It is well-known that the shape and size of surfactant crystals depends on the rate of quench and this is why we expect the quench temperature to have an influence on the final aspect of the gel. These questions will be considered again in section III on the basis of electronic microscope observations.

(4) Water Elimination. The final step to get the macroporous material consists of eliminating the water from the bicontinuous structure. This can be achieved by storing the sample at room temperature and in a dry atmosphere and waiting a sufficient time to allow water evaporation. However, this resulted in the destruction of the gel; under the effect of capillarity, the gel collapses and the final density of the material is close to the one of pure silicone (0.9). In other words, the gel shrinks while water is evaporated and the volume fraction of silicone approaches 90% in the final material. At the macroscopic scale, the dried sample has clearly a smaller volume than the original one. To preserve the structure during the process of water elimination, we followed the method described below. The original gel is quenched in liquid nitrogen and introduced in a chamber connected to a vacuum pump. In such conditions, the frozen water is progressively eliminated through a sublimation process that negligibly perturbs the initial structure of the gel: we can observe that the gel dried through the sublimation process has approximately the same volume as the original one. By simply weighting the sample, we deduce that the average density of the macroporous material varies between 0.15 and 0.25. This confirms that the final silicone volume fraction in the macroporous network lies in the range 20%-30%.

III. Gel Characterization and Discussion

(1) Scanning Electron Microscope (SEM). We observed the dried materials using SEM technique at different levels of magnification. Images on Figure 4 confirm the porous structure, the characteristic pore size being of the order of 10 μm. The microscope resolution is sufficient to observe the partial sintering of the initial silicone droplets: the hemispheres distinguishable on the network surface most probably correspond to droplets from the mother emulsion, which have only partially relaxed their shape (Figure 4d). As discussed in section II.3, we believe that during the cross linking step, a fraction of silicone becomes solid and probably this fraction inhibits the shape relaxation process.

In Figure 4c, the arrow indicates the presence of a needle-shaped crystal of potassium dodecyl sulfate. This could be expected because the addition of potassium iodide produces precipitation of the dodecyl sulfate surfactant. The chemical nature of this crystal is confirmed by X-ray Energy dispersive spectroscopy (EDS). This technique allows measuring the X-ray

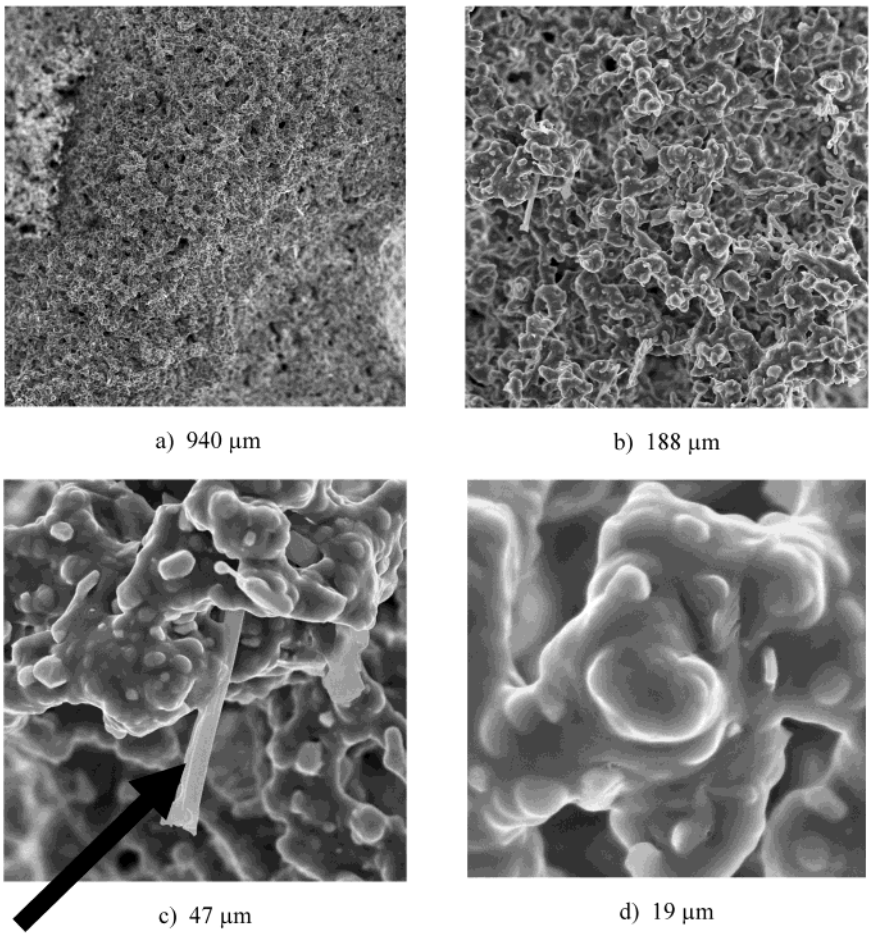

Figure 4. (a)−(d) SEM images of the aerogel at different levels of magnification. Numbers below the images indicate the dimensions of the observed frame. The arrow in (c) indicates the presence of a crystal of potassium dodecyl sulfate.

emission of the atoms of the sample bombarded by the beam of the SEM apparatus. Figure 5a is the EDS spectrum obtained by focusing the incident electronic beam on the crystal observed in Figure 4c. The presence of C, O, S, and K atoms provides convincing evidence for the presence of potassium dodecyl sulfate. Note that the gold (Au) and palladium peaks (Pd) come from the thin conducting layer deposited on the samples prior to the observation. The same type of analysis was performed on the silicone surface (Figure 5b). Potassium dodecyl sulfate is still present but is in relatively small proportions compared to the previous spectrum.

The SEM images reported in Figure 4 correspond to a macroporous aerogel dried following the sublimation process. For the sake of comparison, we report in Figure 6 the image of a gel that was simply dried by evaporation. In this latter case, the topology is completely different, with thicker branches and much smaller amounts of incorporated air. The SEM images perfectly confirm the macroscopic observations: the gel dried following a sublimation process under reduced pressure preserves the initial structure whereas a gel submitted to evaporation at ambient pressure collapses and shrinks. The strong capillary forces induced by water evaporation strongly deform the local structure of the gel and this may induce a considerable increase of the network connectivity. Indeed, because of deformation, some free surfaces may be brought into contact and new anchoring points can be formed. Consequently, the porosity does not remain opened but transforms into a closed one. This is not obvious from the mere images 4 and 6, but we verified that the gel dried under evaporation cannot incorporate water anymore whereas the gel dried under sublimation can. It is also probable that the local rearrangements induced by capillarity produce some further shape relaxation within the interconnected network.

(2) Permeability and Porosity Measurements. We also measured the average porosity of our samples from a very simple experiment. A piece of macroporous aerogel is located at the bottom of a cylindrical glass column (typical radius = 1 cm) filled with pure water (initial water height = $h \approx 100$ cm). The hydrostatic pressure $\Delta P = \rho g h$ ($\rho = 1$ g/cm^3, $g = 9.8$ ms^{-2}; see Figure 7) causes the liquid to flow across the sample at a given velocity v. The relation between ΔP and v is given by the well-known Darcy law:

$$\Delta P = \frac{8\eta L}{\Phi r^2} v$$

in which L is the sample length, η is the water viscosity (10^{-3} Pa·s), Φ is the pore volume fraction (deduced from the density measurements), and r is the average pore radius. In the previous relation, the only unknown parameter is r. By plotting ΔP as a function of v, we get a linear variation and from the slope we deduce the average pore radius r. The curve reported in Figure 8 corresponds to the same aerogel as the one observed in Figure 4. The obtained value for the pore size $r = 5$ μm is in fairly good agreement with the microscopic observations. The same experiment was performed with the sample dried by evaporation. Within exactly the same conditions, we were not able to observe any water flow across the material. This again confirms the presence of closed pores in this aerogel.

In Figure 9, we plot the evolution of the average pore size as a function of the final silicone volume fraction in the aerogel,

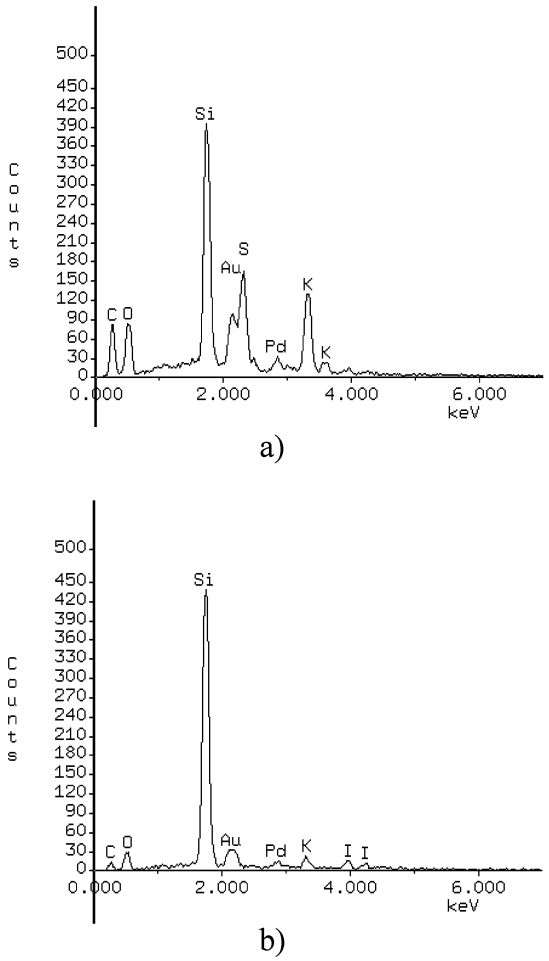

Figure 5. (a) EDS spectrum obtained by focusing the incident electronic beam on the crystal observed in Figure 4c. (b) Same type of analysis performed on the silicone.

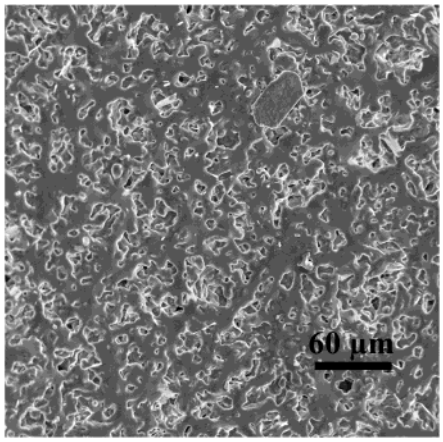

Figure 6. SEM image of a gel that was simply dried by evaporation at room temperature.

ϕ_f. The different gels were obtained by varying the silicone droplet volume fraction in the primary emulsion. After gelation, the samples were cooled in air at room temperature. As could be expected, the average pore size obtained from permeability decreases with the amount of silicone. This is qualitatively confirmed by the SEM images of Figure 10. The silicone volume fraction in the final gel increases from approximately 10% in (a) to 40% in (d). The gel corresponding to (d) is composed of clusters that are larger and more compact than in Figure 10a. At the same time, the characteristic distance separating the clusters seems to decrease from (a) to (d), in agreement with the permeability measurements.

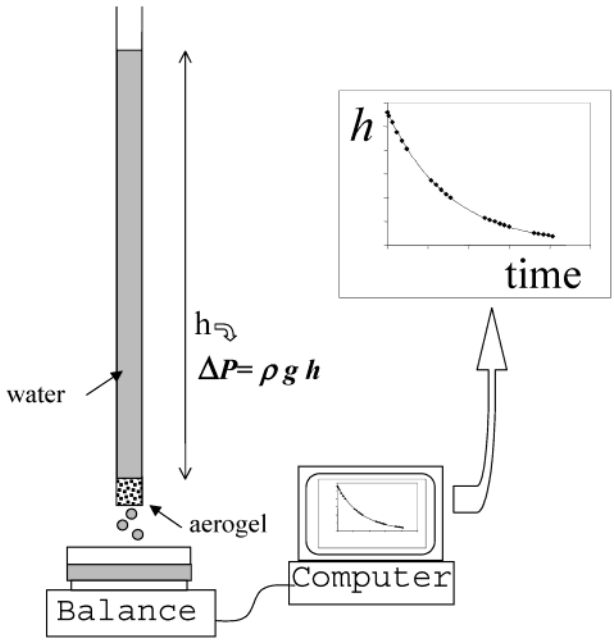

Figure 7. Sketch of the setup used to measure the porosity of the gel.

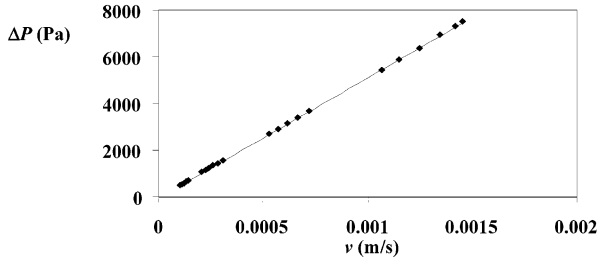

Figure 8. Measured water flow rate through the macroporous aeerogel as a function of the hydrostatic pressure.

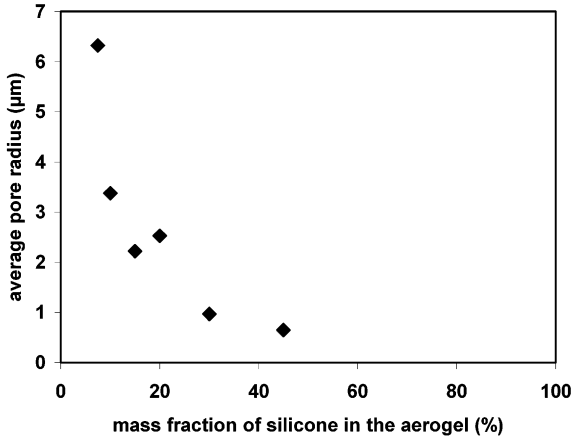

Figure 9. Measured average pore size obtained from permeability as a function of the final silicone volume fraction in the aerogel.

(3) Mechanical Properties and Potential Applications of the Macroporous Silicone Aerogels. Our macroporous gels exhibit elastic behavior. They can be reversibly compressed or elongated many times without any distortion in their initial shape. Moreover, their rigidity (elastic modulus) can be varied by tuning the final gel volume fraction. As previously described, this parameter can be easily varied via the temperature quench (after KI addition) or via the silicone volume fraction in the mother emulsion.

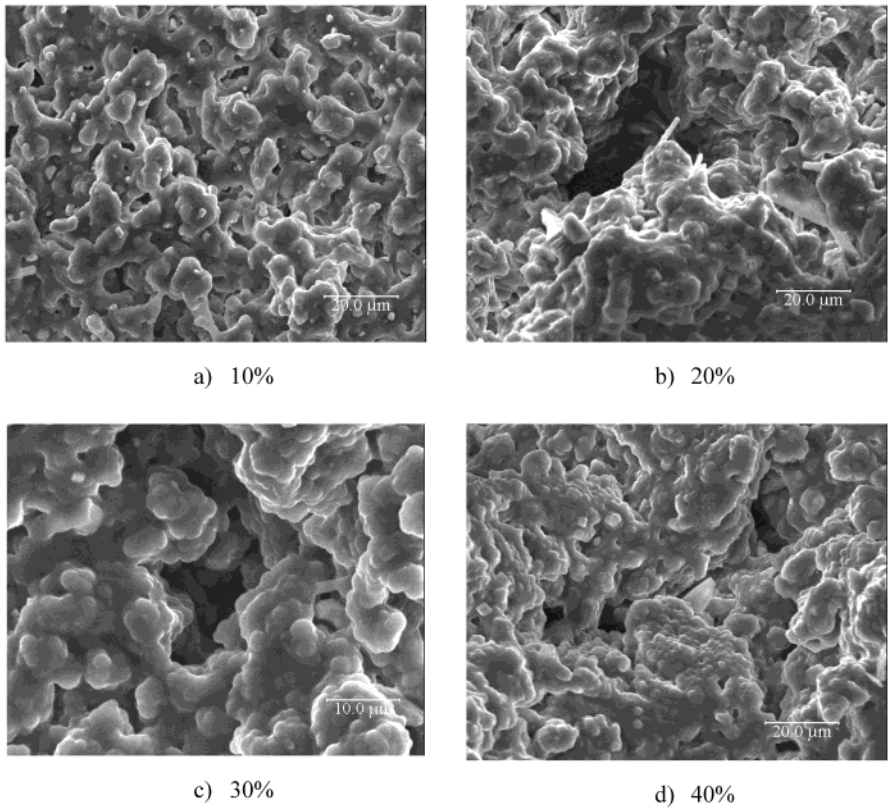

Figure 10. SEM images of the gels obtained at different final silicone fractions: (a) $\phi_f \approx 10\%$; (b) $\phi_f \approx 20\%$; (c) $\phi_f \approx 30\%$; (d) $\phi_f \approx 40\%$.

The silicone macroporous aerogels offer interesting possibilities in terms of practical applications. Among the many different potential applications, we can mention

filtration membranes
industrial wrappings
artificial skins
hydrophobic coatings
catalytic beads

The last application requires chemical functionalization of the gel surface, which seems possible due to the presence of OH groups at the silicone surface. Silicone aerogels are permeable to oxygen and water vapor, and due to their chemical inertia, they could be used for medical purposes such as artificial skins or human implants. The homothetic contraction preserves the shape of the gel and consequently it becomes very easy to produce materials with well-defined size and geometry. Current investigations are devoted to produce mixed aerogels in the presence of mineral particles (silica, aluminum oxide, hydroxyl apatite, etc). By combining silicone and solid mineral particles, we expect to get new materials with enhanced mechanical properties (rigidity, resistance to water evaporation, etc.).

IV. Conclusion

In this paper, we have presented experimental evidence for viscous sintering phenomena in an emulsion composed of highly viscous silicone droplets dispersed in water. After appropriately removing the water, we obtain a light macroporous aerogel. The method that was described here is interesting because it allows transforming an initially liquid emulsion into a rigid and porous material within a short period of time and at room temperature. The sintering process that was applied to a silicone emulsion can be extended to other polymerizable oils and may become a novel route to easily produce light and resistant materials.

Acknowledgment. This work was financially supported by the Rhodia Company. We thank P. Maestro for constant encouragements and Y. Giraud for fruitful discussions.

References and Notes

(1) Ostwald, W. *Z. Phys. Chem.* **1901**, *37*, 385.
(2) Deminière, B.; Colin, A.; Leal-Calderon, F.; Bibette, J. *Phys. Rev. Lett.* **1999**, *82*, 229.
(3) Frenkel, J. *J. Phys.* **1945**, *9*, 385.
(4) Binder, K.; Stauffer, D. *Phys. Rev. Lett.* **1974**, *33*, 1006.
(5) Philip, J.; Bonakdar, L.; Poulin, P.; Bibette, J.; Leal-Calderon, F. *Phys. Rev. Lett.* **2000**, *84*, 2018.
(6) Mackenzie, J. K.; Shuttleworth, R. *Proc. Phys. Soc. London* **1949**, *62*, 833.
(7) Scherer, G. W. *J. Am. Ceram. Soc.* **1977**, *60*, 236.
(8) Scherer, G. W. *J. Am. Ceram. Soc.* **1977**, *60*, 243.
(9) Mabille, C.; Schmitt, V.; Gorria, P.; Leal Calderon, F.; Faye, V.; Deminière, B.; Bibette, J. *Langmuir* **2000**, *16*, 422.
(10) Scherer, G. W. *J. Am. Ceram. Soc.* **1991**, *74*, 1523.
(11) Scherer, G. W.; Brinker, C. J.; Roth, P. E. *J. Non Cryst. Solids* **1985**, *72*, 369.
(12) Scherer, G. W. in *Surface & Colloid Science*; Matijevic, E., Ed.; Plenum Press: New Jersey, 1987; Vol. 14.
(13) Poulin, P.; Bibette, J. *Phys. Rev. Lett.* **1997**, *79*, 3290.
(14) Poulin, P.; Nallet, F.; Cabane, B.; Bibette, J. *Phys. Rev. Lett.* **1996**, *77*, 3248.
(15) Poulin, P. Thesis: Adhesion phenomena in emulsions 1995, University of Bordeaux I.